Pressure Effects in Differential Mobility Spectrometry

ARTICLE *in* ANALYTICAL CHEMISTRY · DECEMBER 2006

Impact Factor: 5.64 · DOI: 10.1021/ac061092z · Source: PubMed

5 AUTHORS, INCLUDING:

Erkinjon G. Nazarov
Draper Laboratory
93 PUBLICATIONS **2,255** CITATIONS
SEE PROFILE

Stephen L. Coy
Massachusetts Institute of Technology
94 PUBLICATIONS **1,752** CITATIONS
SEE PROFILE

Evgeny V Krylov
908 Devices Inc.
50 PUBLICATIONS **1,460** CITATIONS
SEE PROFILE

Anal. Chem. **2006,** *78,* 7697−7706

Pressure Effects in Differential Mobility Spectrometry

Erkinjon G. Nazarov,*,† Stephen L. Coy,† Evgeny V. Krylov,† Raanan A. Miller,† and Gary A. Eiceman‡

Sionex Corporation, 8-A Preston Court, Bedford, Massachusetts 01730, and New Mexico State University, Las Cruces, New Mexico 88003

A microfabricated planar differential ion mobility spectrometer operating from 0.4 to 1.55 atm in a supporting atmosphere of purified air was used to characterize the effects of pressure and electric field strength on compensation voltage, ion transmission, peak width, and peak intensity in differential mobility spectra. Peak positions, in compensation voltage as a function of separating rf voltage, were found to vary with pressure in a way that can be simplified by expressing both compensation and separation fields in Townsend units for *E/N*. The separation voltage providing the greatest compensation voltage and the greatest resolution is ion-specific but often occurs at *E/N* values that are unreachable at elevated pressure because of electrical breakdown. The pressure dependence of air breakdown voltage near 1 atm is sublinear, allowing higher *E/N* values to be reached at reduced pressure, usually resulting in greater instrumental resolution. Lower voltage requirements at reduced pressure also reduce device power consumption.

Differential mobility spectrometry (DMS)[1] expands the capabilities of ion mobility spectrometry (IMS) by extending ion characterizations over a broad range of electric field strengths. In DMS, the changes in ion mobility are measured through a range of field strengths yielding a function that describes the field variation of mobility. Mobility measurements in conventional IMS studies are limited to low-field conditions. Developed and refined over the past decade, DMS is also known as field ion spectrometry[2] and field-asymmetric waveform ion mobility spectrometry.[3] Several configurations of DMS analyzers have shown response at ambient pressure, often in air, to trace amounts of chemical species,[4] including explosives,[5] chemical warfare agents simulants,[6] toxic chemicals,[7] and a variety of other organic[8] and inorganic[9] substances. Hybrid DMS techniques can provide detection and identification of biological materials.[10−13]

Ion separation at ambient pressure in DMS is based on the nonlinear dependence of the mobility coefficient $K(E)$ on an electric field as large as 30 000 V/cm (eq 1).[1,14,15]

$$K(E) = K(0)[1 + \alpha(E/N)] \cong K(0)[1 + \alpha_2(E/N)^2 + \alpha_4(E/N)^4 + ...] \quad (1)$$

where $K(0)$ is the mobility coefficient for electric fields below 10 Td (2400 V/cm at 1 atm), α_i parameters are functions that describe the dependence of K on the electric field, and N is the total gas density (in molecules/cm^3). The physical meaning of the α parameter is clarified in eq 1a:

$$\alpha(E/N) = \frac{K(E) - K(0)}{K(0)} = \frac{\Delta K(E)}{K(0)} \quad (1a)$$

An α parameter describes changes in the mobility coefficient with electric field strength at the same density of the supporting atmosphere. The α parameter may be positive or negative in sign, and this discloses the direction of change in the coefficient of mobility (and compensation voltage) as E is changed at constant N.[16]

The goal of this work is to investigate the effect of the E/N parameter on the DMS spectra and to determine the possibility

* Corresponding author.Phone: 781 457 5413. E-mail: Egnazarov@Sionex.com.
† Sionex Corp.
‡ New Mexico State University.

(1) Buryakov, I. A.; Krylov, E. V.; Nazarov, E. G.; Rasulev, U. Kh. *Int. J. Mass Spectrom.* **1993**, *128*, 143−8.
(2) Carnahan, B.; Day, S.; Kouznetsov, V.; Matyjaszczuk, M.; Tarassov, A. Proceeding of the International Conference on Advance in Instrumentation and Control, ISA, 1996; pp 87−95.
(3) Purves, R. W.; Guevremont, R.; Day, S; Pipich, C. W; Matyjaszczyk, M. S. *Rev. Sci. Instrum.* **1998**, *69*, 4094−105.
(4) Miller, R. A.; Eiceman, G. A.; Nazarov, E. G.; King, A. T. *Sens. Actuators, B* **2000**, *67*, 300−6.
(5) Eiceman, G. A.; Krylov, E. V.; Krylova, N. S.; Nazarov, E. G.; Miller, R. A. *Anal. Chem.* **2004**, *76*, 4937−44.
(6) Krylova, N.; Krylov, E.; Stone, J. A.; Eiceman, G. A. *J. Phys. Chem.* **2003**, *107* (19), 3648−54.
(7) Eiceman, G. A.; Nazarov, E. G.; Tadjikov, B.; Miller, R. A. *FACT* **2000**, *4* (6), 297−308.
(8) Eiceman, G. A.; Tadjikov, B.; Nazarov, E. G.; Miller, R. A.; Westbrook, J.; Funk, P. *J. Chromatogr., A* **2001**, *917*, 205−17.
(9) Eiceman, G. A.; Tarassov, A.; Nazarov, E. G.; Hughes, E.; Funk, P. *J. Sep. Sci.* **2003**, *26*, 585−93.
(10) Eiceman, G. A.; Nazarov, E. G.; Miller, R. A.; Krylov, E. V.; Zapata, A. *Analyst* **2002**,*127*, 294−304.
(11) Schmidt, H.; Tadjimukhamedov, F.; Mohrenz, I. V.; Smith, G. B.; Eiceman, G. A. *Anal. Chem.* **2004**, *76*, 5208−17.
(12) Krebs, M. D.; Zapata, A. M.; Nazarov, E. G.; Miller, R. A.; Costa, I. S.; Sonenshein, A. L.; Davis, C. E. *IEEE Sens. J.* **2005**, *5* (4), 4937−44.
(13) Tang, K.; Shvartsburg, A. A.; Strittmatter, E. F.; Smith, R. D. *Anal. Chem.* **2005**, *77*, 6381−8.
(14) McDaniel, E. W.; Mason E. A. In *The Mobility and Diffusion of Ions in Gases*; Brown, S. C., Ed.; Wiley: New York, 1973; p 372.
(15) Mason, E. A. In *Plasma Chromatography*; Carr, T. W., Ed.; Plenum Press: New York, 1984; Chapter 2, p 49.
(16) Miller, R. A.; Nazarov, E. G.; Eiceman, G. A.; King, T. *Sens. Actuators, A* **2001**, *91*, 301−32.

10.1021/ac061092z CCC: $33.50
Published on Web 10/20/2006

of using pressure with electric field strength (as E/N) for enhanced performance of a DMS analyzer. Since E/N can be changed by varying electric field or neutral gas density (pressure), in this work, DMS spectra were obtained for different pressures with various rf voltages spanning as large a range as technically possible. The findings may provide a new understanding of the role of pressure on ion formation and dissociation and the effect of pressure on separation in DMS. The practical values of such studies would be the identification of optimal regimes of operation for planar DMS analyzers. Finally, the effect of pressure on DMS performance has a special interest for DMS prefiltering of ions at atmospheric or reduced pressure for mass spectrometric analysis.[17,18] The compact "invisible" planar DMS with low power consumption can be maintained in the mass spectrometer interface area providing reduced spectral complexity and chemical noise, significantly enhancing the mass spectrometric results.

PRINCIPLES OF ION BEHAVIOR IN A DIFFERENTIAL MOBILITY SPECTROMETER

The operating principles for a DMS analyzer have been previously described in detail,[1−4] but we provide a brief description for completeness. Ion analysis and separation occurs as ions are moved in a flow of gas between two parallel metal plates that are used to develop, perpendicular to the gas flow, an electric field up to 30 kV/cm. The field consists of an asymmetric-waveform rf separation field (V_{rf}) combined with a weaker dc compensation field (V_C). The asymmetric rf field develops oscillations in the motion of the ions flowing between the plates. In general, the repeated oscillations of ions between the plates results in a displacement toward one plate since ion displacements are not equal during the forward and return cycles of the waveform due to speed changes caused by field variations in the ion mobility, $K(E)$, as suggested by eq 2 for the ion velocity:

$$\bar{\vartheta}(t) = K(\vec{E}(t))E(t) \tag{2}$$

The rf waveform $E(t)$ will yield no net displacement if K is the same at all field strengths. When mobility coefficients $K(E)$ are nearly unchanged by changes in field strength, ions will pass through the narrow channel between the electrodes at a compensation voltage at or near zero volts. In order to pass through the channel, the period average of ion velocity perpendicular to the flow direction must be zero; i.e., $\langle \vartheta(t) \rangle = 0$. If an ion has some net lateral displacement (i.e., $\langle \vartheta(t) \rangle \neq 0$), the ion will collide after some number of cycles with one of the electrodes an will be neutralized. The lateral displacement of an ion through the analytical gap can be adjusted to zero by imposing a dc potential, or compensation voltage (V_C), on the plate with a power supply that is decoupled from the rf generator. A scan of the compensation voltage with time is used to produce a DMS spectrum as ion species are passed at specific V_C through the analyzer and to a detector where current is produced by ion collection at the detector. The V_C scan rate is made slow enough that ions experience a constant value during the ion residence time in the analytical region. The residence time is usually on the order of milliseconds, but may be adjusted up or down based on the required resolution through changes in channel geometry or in flow rate. Thus, the DMS method provides information about the direction and magnitude of changes in the coefficient of mobility as a function of E. In contrast, the well-known IMS technique measures the low-field absolute value of ion velocity in a dc electric field.[19,20] Therefore, the analytical parameter is drift time for an ion swarm in IMS and is compensation voltage for ion passage through the plates in DMS. Common to both methods is ion characterization based on ion velocity. In DMS, the trajectory of ions is a function of differences in velocities in the high- and low-field portions of the asymmetric waveform, and in IMS, the ion species is determined by the drift time $t_d = l/\vartheta_d$, where l is the drift region length and ϑ_d is the ion swarm velocity.

Ion velocity is a shared feature of DMS and IMS. Ion motion under effect of electric field in IMS-based systems can be understood by rearrangement of the following equation often used in mobility measurements for velocity of ion swarms.[14,15]

$$\vartheta = KE = \frac{3q}{16}\left(\frac{2\pi}{\mu kT}\right)^{1/2}\frac{1+\zeta}{\Omega(T)}\left(\frac{E}{N}\right) \tag{3}$$

In eq 3, μ is the ion-neutral reduced mass, q the ion charge, T the effective temperature, $\Omega(T)$ the ion-neutral cross section, ζ a small correction term, and N the gas density, which can be converted to pressure using $N = P/kT$. For a fixed temperature, we see that the velocity of the ion swarm depends linearly on E/N if the mass and cross section of ions do not change. Ion velocity may be influenced independently by either electric field or gas pressure through the ratio of E/N. This has been observed in recent descriptions of the effect of pressure in IMS[21,22] with conventional designs of drift tubes with moderate electric fields of ~200 V/cm. Linear dependence of drift velocity on E/N was observed in the region of 0.04−1 atm for relatively small ions such as hydrated proton clusters, $(H_2O)_2H^+$ and $(H_2O)_3H^+$ (37 and 55 Da), nitric oxide, NO^+, (30 Da), protonated monomer for ethyl acetate, MH^+, (89 Da), and for somewhat larger ions: protonated monomers for amyl acetate (131 Da), methyl isobutyl ketone (101 Da), and the proton-bound dimer of methyl isobutyl ketone (201 Da) and methyl salicylate (152 Da). However, some nonlinearity in the coefficient of mobility with pressure was observed in this traditional technology below 30 Torr when E/N exceeded 20 Td, particularly for low-mass ions.

Since E/N in DMS can reach very high values (up to 200 Td), consideration should be given to the collision process during ion motion to clarify causes of the field dependence of mobility. Gaseous ions in an electric field accelerate between collisions gaining energy $\epsilon_i = q\lambda E$ from the applied electric field through the distance between collisions, the free mean path, λ. The mean

(17) Barnett, D. A.; Ells, B.; Purves, R. W.; Guevremont, R. *J. Am. Soc. Mass Spectrom.* **2003**, *13*, 1282−91.

(18) Shvartsburg, A. A.; Li, F.; Tang, K.; Smith, R. D. *Anal. Chem.* **2006**, *78*, 3706−14.

(19) Eiceman, G. A.; Karpas, Z. *Ion Mobility Spectrometry*, 1st ed.; CRC Press: Inc.: Boca Raton, FL, 1994; Vol. 1, p 228.

(20) Eiceman, G. A.; Karpas, Z. *Ion Mobility Spectrometry*, 2nd ed.; Taylor & Francis/CRC Press: Boca Raton, FL, 2005; p 350.

(21) Bensch, H.; Rodolph, P. The influence of pressure variation on the peak shape of ion mobility spectra, ISIMS 2005, poster.

(22) Tabrizchi, M.; Rouholahnejad, F. *J. Phys. D Appl. Phys.* **2005**, *38*, 857−62.

free path depends on cross section of the ion−molecular pairs and neutral density or gas pressure as in eq 4:

$$\lambda \propto 1/\Omega N \tag{4}$$

Energy gained between collisions is partially or completely lost at the next collision and the ion is again accelerated before a subsequent collision. Equilibrium is reached when the average energy $\Delta\epsilon_i$ gained between collisions is the same as the energy lost ($-\Delta\epsilon_i$) through collisions and the conditions of eq 2 are established. This mechanism for transfer of electric field energy to the gas is general and was described by Wannier,[23] who showed that the mean energy gained by ions in an electric field is distributed in three forms: gas temperature kT, ion kinetic energy (third term), and kinetic energy of gas molecules (second term) located close to ion trajectories as in eq 5

$$\bar{\epsilon}_i = \frac{3}{2}kT + \frac{M\vartheta_i^2}{2} + \frac{M_i\vartheta_i^2}{2} \tag{5}$$

Thus, the partition of acquired ion energy depends upon ion mass M_i and mass of molecules in the supporting atmosphere, M. When molecules and ions have the similar masses, ϵ_i is equally distributed between ions and molecules. For heavy ions, $M_i \gg M$ and the energy gained from the electric field remains principally in ion motion. In contrast, light ion motion amid large molecules media results in increased kinetic energy (temperature) of the gas molecules.

DMS methods are based upon a nonlinear field dependence of ion velocity that results from field-induced changes in the mean free path and cross sections.[24,25] The field dependence of mobility may be understood as arising through several mechanisms.[14,15,26]

(1) Elastic Scattering due to Polarization Interaction.[27] When ions move slowly in gases ($\Delta\epsilon_i \leq kT$), polarization of the gas molecules near ions occurs. The effective ion-neutral cross section (Ω_{pol}) is determined by the strength of polarization forces as measured by the capture cross section and depends on kinetic energy of ions.[28,29] As ion velocity increases, the distance of capture decreases since the polarization cross section is inversely related to ion velocity (energy) $\Omega_{pol} \sim 1/(\epsilon_i)^{1/2}$. When the effective radius of polarization forces decreases to the molecular geometric size, the effective cross section decreases to the constant gas kinetic cross section, which is less than polarization cross section $\Omega < \Omega_{pol}$. Usually this occurs when the energy of ions becomes higher than thermal energy $\bar{\epsilon}_i > 0.5$ eV. This can explain the increase of K with E through a change from a large polarization cross section to smaller rigid-sphere value and would explain ion behavior in nonpolar gases.

(2) Resonant Charge Transfer.[26,29] When ions move in a gas containing neutral molecules similar in structure to the ions, the transfer of an electron from an ion to a neutral occurs easily. Due to the resonant nature of this process, charge transfer happens so quickly that the newly formed ion has greatly diminished drift velocity and begins acceleration from zero velocity, which could decrease the coefficient of mobility. The cross section for charge transfer is usually even greater than the elastic scattering cross section and leads to reduced ion mobility with increased electric field.

(3) Scattering due to Direct "Contact". Wannier[14,23] showed that, with rigid-sphere ion-neutral interaction and resonant charge transfer, at moderate values of E, drift velocity is proportional to $\vartheta_d \sim E/N$, but with increasing electric field dependence gradually becomes $\vartheta_d \sim (E/N)^{1/2}$. This arises in eq 3 when the cross section becomes constant and the effective temperature is dominated by field acceleration.

(4) Clustering and Declustering of Ions.[6] Under the strong nonsymmetric waveform electric field, collision cross sections of ions may be altered due to changes in the degree of solvation during different portion of rf voltage. In the low-voltage portion of the rf period, ions have a higher level of solvation than during the strong electric field cycle where the level of solvation decreases due to increases in ion temperature. In this case, the high-field coefficient of mobility corresponds to smaller mass and smaller effective cross section ($\mu(t)$,$\Omega(t)$) during some parts of the rf cycle.[6]

(5) Change in Shape due to Ion Effective Temperature or Strong rf Electric Field. Changes in the shape of a molecule due to high temperature has been theoretically predicted and experimentally observed. The strong rf field in DMS creates a high effective temperature that could change the molecular conformation. The electric field in portions of the asymmetric waveform may reach 30 000 V/cm corresponding to effective temperatures well above kT. This could modify conformations and dipole moments of ion complexes.[30]

These several phenomena may account for the unique dependences of mobility of ions with E/N and provide a set of principles to rationalize empirical trends. As of yet, there are very few integrated models with interpretative or predictive capabilities for a broad range of sizes, structures, or functional groups of ions mobility.[31]

EXPERIMENTAL SECTION

Instrumentation. The differential mobility spectrometer is a Sionex Corp. model SVAC (Bedford, MA) in the arrangement of flows shown in Figure 1. The dimensions of the plates in the DMS analyzer are as follows: length, 15.0 mm; width, 1.5 mm; and gap, 0.50 mm. The width of the channel established for ion flow is restricted to 1.0 mm, aligned to the center of the plates. The volume between the plates is 7.5 mm^3, so that with the usual transport gas flow rate of 0.3 L min^{-1} the residence time of an ion in the analytical volume is ~1.5 ms. The electric field established by an asymmetric waveform was as follows: rf frequency, 1.18 MHz; and duration of positive polarity, 0.25 from rf period (T). The waveform shape was unchanged for peak

(23) Wannier, G. H. *Bell Syst. Tech. J.* **1953**, *32*, 170.
(24) Ellis, H. W.; Pai, R. Y.; McDaniel, E. W.; Mason, E. A.; Viehland, L. A. *At. Data Nucl. Data Tables* **1976**, *17*, 177−210.
(25) Viehland, L. A.; Mason, E. A. *At. Data Nucl. Data Tables* **1995**, *60*, 37−95.
(26) Mason, E. A.; McDaniel, E. W. *Transport Properties of Ions in Gases*; Wiley: New York, 1988.
(27) Langevin, P. *Ann. Chim. Phys.* **1905**, *5*, 245.
(28) Gioumousis, G.; Stevenson, D. P. *J. Chem. Phys.* **1958**, *39*, 294.
(29) Mason, E. A.; McDaniel, E. W. *Transport Properties of Ions in Gases*; Wiley: New York, 1988; p 245.
(30) Ferrara, P.; Apostolakis, J.; Caflisch, A. *J. Phys. Chem. B* **2000**, *104*, 5000.
(31) Kim, H.; Kim, I. H.; Beegle, L. W.; Johnson, P. V.; Beauchamp, J. L.; Kanik, I. Theoretical Ion Mobility Studies of Amino Acids. Lunar and Planetary Science Conference XXXVII, Lunar and Planetary Institute, Houston, TX, 2006; Abstract 2127.

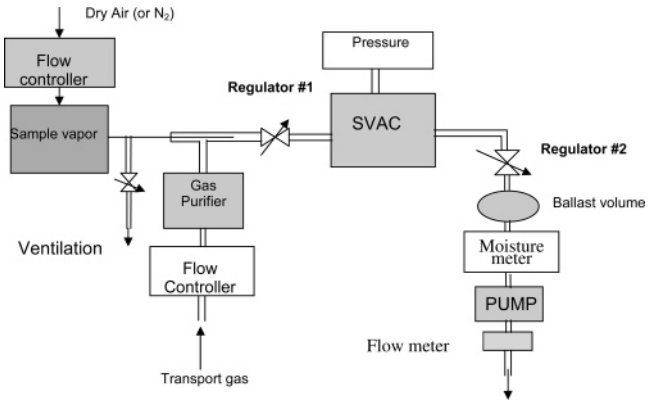

Figure 1. Schematic instrumentation for studies from 0.4 to 1.55 atm pressure of supporting atmosphere inside the DMS analyzer.

amplitudes from 500 to 1500 V, and the corresponding peak electric field in the analytical gap was 10 000−30 000 V/cm.

Air was purified and used as the transport gas to move ions through the analyzer. Air was cleaned using a Drierite Gas Purifier (W.A. Hammond Drierite Co., Ltd., Xenia, OH). A stable flow of vapor samples (of dimethyl methyl phosphonate (DMMP) or methyl salicylate (MS)) was provided by two independently operated model 190 Dynacalibrator calibration gas generators (VICI Metronics Inc., Poulsbo, WA). A flow of dried nitrogen at 5 L/min was passed through the permeation tube chamber; permeation tubes were provided by Kin-Tek Laboratories, Inc. (LaMarque, TX). The generator chamber was 110 °C for DMMP and 80 °C for MS. A small portion (3−35 mL/min) of total gas flow from the gas generator was introduced into the DMS analyzer. A DMS analyzer was joined to a mass spectrometer in a way based on the interface previously described.[32] In current work, the mass spectrometer was an AccuTOF JMS-T100LC time-of-flight mass spectrometer (JEOL, Peabody, MA). In MS experiments, the flow and sample delivery system was similar to that in Figure 1.

In DMS analyzers, a radioactive β source (^{63}Ni) is used for sample ionization just before the entrance of the DMS analytical gap. Electron-impact ionization occurs due to collision of high-energy β particles emitted from the source. In air, ions of nitrogen and oxygen as well as free electrons and thermoelectrons are generated in the reaction region by the direct impact of β-electrons with air molecules. Ion−molecule interaction at elevated pressure conditions the positive $\{H^+(H_2O)_n\}(N_2)_m\}$ and negative $\{O_2^-(H_2O)_n\}$ reactant ions are formed. In the absence of analyte molecules, formed reactant ions pass through the analytical gap of DMS practically without any chemical reactions and are recorded as reactant ion peaks in DMS spectrum. When analyte molecules (M) from the sample are introduced into the reaction region, reactant ions undergo collisions with these analyte molecules and could form analyte ions in positive $\{MH^+(H_2O)_{n-1}\}$ or in negative mode $MO_2^-(H_2O)_{n-1}$. Efficiency of formation positive and negative ions and level of clusterization of formed ion species depends on energetic properties of analyte molecules, the level of humidity, and the concentration of analyte molecules. Gas-phase ion chemistry of ions species formation in IMS and DMS systems in details is described in chapter 3 of ref 20.

(32) Eiceman, G. A.; Nazarov, E. G.; Miller, R. A. *Int. J. Ion Mobility Spectrom.* **2000**, *3*, 15−27.

Procedures. Sample Introduction and Pressure Control. The concentration of sample vapors after dilution in transport gas was 4.6 ppb_v for DMMP and 0.5 ppb_v for MS. Pressure readings were obtained directly from the Sionex SVAC, which provides a pressure reading from a sensor on the input to the analyzer. Needle valves (no. 1 and 2 in Figure 1) were regulated to control pressure inside the analyzer from 0.4 to 1.5 atm while the total transport gas flow was kept constant at 300 mL/min. A flow meter located on the exhaust of a miniature pump (KNF Neuberger Inc., serial 4800-088) measured the total transport gas flow rate. The maximum moisture at the lowest pressure was 30 ± 5 ppm and at the highest pressure it was ~20 ppm. Moisture was measured at the exhaust of DMS sensor. To avoid introducing impurities, flow meters were excluded from the sample delivery lines. Sample flow rate was determined by subtracting the value of transport gas line flow from total flow meter reading and was kept constant. The transport gas flow controller was mounted before a molecular sieve filter. Supply lines after the vapor generator were kept at 50 °C to minimize sample wall adsorption. The diffusion or permeation tubes were weighed over several weeks to determine gravimetrically concentrations in the sample flows.

Mass Spectrometry Identification of Ions in Differential Mobility Spectra. In the DMS/MS interface, one of the detectors of the DMS was modified to function as a deflector electrode to direct ions, after DMS selection, toward the opposite detector plate modified with a 2-mm-diameter hole. Ions were directed through this hole into the orifice of the mass spectrometer. Metering valves located before (valve 1) and after the DMS analyzer (valve 2) allowed control of pressure in the analytical gap. Software for the DMS allows control and scanning of compensation and separation voltages, setting the conditions to pass selected ions into the mass spectrometer. The planar DMS design, in contrast to the cylindrical design,[33] maintains low peak width at all field settings, permitting a complete resolution by MS of all ion species formed in the ionization region.[18] When the rf separation voltage generator is off and the compensation voltage set to zero, the mass spectra of all ions formed in the ionization region are obtained.

Data Acquisition and Processing. Commercially provided software with the Sionex SVAC analyzer permitted DMS spectra to be recorded, stored, and displayed for positive and negative ions simultaneously. Spectra could be displayed as line spectra of detector current versus compensation voltage or as topographic plots scanned in both compensation and separation voltages. This latter option permits the creation of dispersion plots (topographic view of current for (V_C, V_{rf}) values) that can disclose ion transformations with changes in rf voltage. The dispersion plots are generated by stepping the separation voltage (V_{rf}) as compensation voltage (V_C) was scanned between −35 and 10 V, stepping separation voltage each second. The range of V_{rf} was nominally 500−1500 V in 10-V steps, and the total time to generate each dispersion plot was 100 s. Additional processing was performed using IGOR Pro (Wavemetrics Inc., Lake Oswego, OR). This software was used to display experimental dispersion plots on the same screen for comparative analysis of large set experimental data, to extract a certain spectrum from all data sets, and

(33) Guevremont, R.; Purves, R. W. *Rev. Sci. Instrum.* **1999**, *70*, 1370−83.

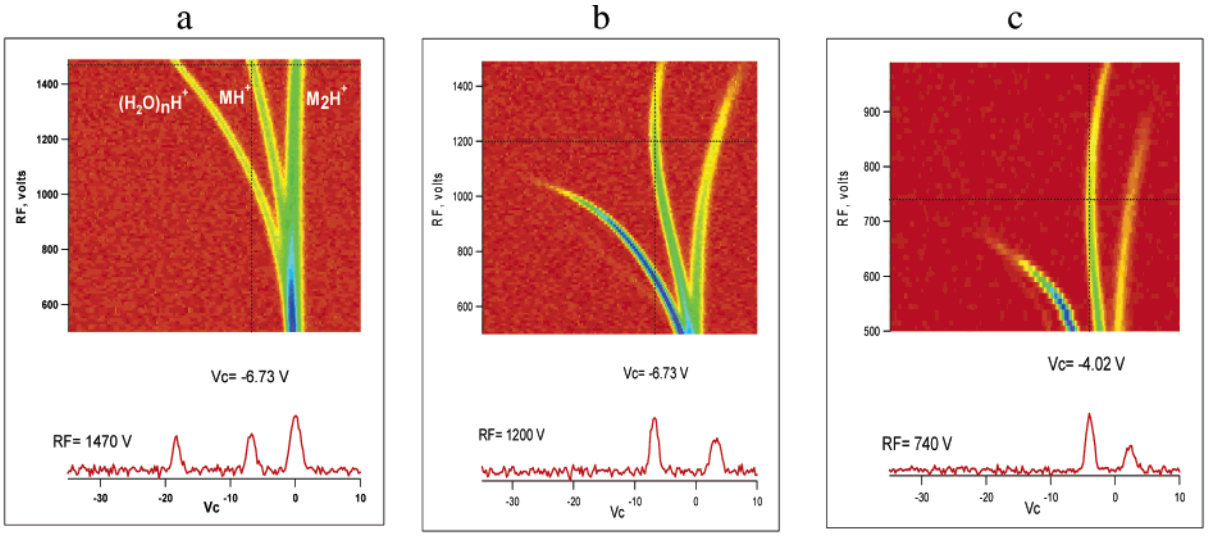

Figure 2. Dispersion curves for effect of pressure on DMS response to DMMP at pressures of 1.55 (a), 0.76 (b), and 0.42 atm (c). Spectra shown below were isolated at separation rf voltages of 1470, 1200, and 740 V, respectively.

also to extract the α function.[34] In addition, Origin (OriginLab Corp., Northampton, MA) software was used for smoothing spectra and deconvolving particular peaks in the DMS spectra.

RESULTS AND DISCUSSION

Pressure Effects in Differential Mobility Spectra for Dimethyl Methyl Phosphonate. Dispersion plots are shown in Figure 2 for DMMP at 4.6 ppb in air at pressures of 1.55, 0.76, and 0.42 atm. In a dispersion plot, differential mobility spectra are obtained through a range of separation fields, scanned here from 500 to 1500 V for 1.55 and 0.76 atm or to 1000 V for 0.42 atm. Ion intensity and compensation voltage at each separation field are seen in the dispersion plots, which also provide a measure of field dependence of mobility for all ions through tracks as seen in Figure 2.

Each track can be associated with an ion and these were identified as the positive reactant ions, the protonated monomer, $(DMMP)H^+$ (125 Da), and the proton-bound dimer $(DMMP)_2H^+$ (249 Da). Reactant ions in purified air are hydrated protons, $H^+(H_2O)_n$, where n is governed by temperature and moisture level and was calculated as 75% for $n = 3$ and 25% for $n = 4$.[35] These ion identities are based on previous DMS/MS experiments. The current mass spectrometer measurements were at lower sub-ppm moisture levels and observed $n = 1$, $n = 2$, and some HN_2^+. The shape and location of tracks in each plot and comparisons between plots demonstrate that each ion exhibits a distinctive dependence on separation field and importantly, for this study, that pressure affects the differential mobility of these ions. Differential mobility spectra (compensation voltage scans at fixed separation voltages) are shown below the dispersion plots for selected separation voltages providing a preliminary measure of the influence of pressure on DMS spectra.

Plots of peak position, as compensation voltage, against separation voltage for nine pressures between 1.55 and 0.42 atm are shown in Figure 3 for protonated monomer and proton-bound dimer peaks of DMMP. Differences exist between these ions at a given pressure in both V_C and the pattern of change of V_C with V_{rf}.

The relationship between V_C and V_{rf} is changed by pressure. At elevated pressures where P > 1 atm, the protonated monomer peak shifts monotonically toward negative V_C up to 1500 V for V_{rf}. At lower pressures, $P \leq 1$ atm, V_C is not a monotonic function of V_{rf} and a maximum in $|V_C|$ is seen. With decreasing pressure, the bend in the curve occurs at progressively lower V_{rf} values and the overall maximum value of compensation voltage, $\max|V_C|$, becomes lower than at higher pressures. For example, the value of $\max|V_C|$ at 0.86 atm differs from a value at 0.42 atm by nearly 2-fold (−7.5 and −4 V, respectively). Moreover, the protonated monomer peak position crosses a compensation voltage of 0 V at increased V_{rf}, revisiting the condition when rf = 0 V as shown in Figure 3. For example, the value of $V_C \sim -1$ V for 0.6 atm (curve on 0.7) at 500 V, reaches a maximum value of $\max|V_C| = -6$ V at 1000 V and is $V_C = 0$ V at 1400 V. The effects of pressure on the proton-bound dimer differed from that of the protonated monomer and this is seen also in Figure 3 where peak behavior is monotonic throughout all values of V_{rf} at all pressures. Pressure effects become significant at low pressures where V_C is displaced to increasingly positive V_C values with decreases in pressure. This behavior for DMMP cluster ions is the same as was observed for ketone cluster ions.[34]

These trends in compensation voltage with pressure and separation voltage are clarified in differential mobility spectra shown in Figure 4. Differential mobility spectra at V_{rf} of 1000 V are shown for pressures from 0.4 to 1.5 5 atm in the left frame. Monomer peak positions (V_C), peak intensities, peak widths (fwhm), and dimer/monomer ratio are plotted in the right frame of Figure 4. These plots suggest that different pressure values should be chosen for the highest sensitivity than for the best resolution. Pressures between 0.8 and 1 atm provide the greatest intensities while the greatest compensation voltages occur from 0.6 to 0.8 atm. On the basis of these considerations, we suggest that the optimum pressure for DMMP samples is ~0.8 atm. At

(34) Krylov, E.; Nazarov, E. G.; Miller, R. A.; Tadjikov, B.; Eiceman, G. A. *J. Phys. Chem. A* **2002**, *106*, 5437−44.

(35) Kebarle, P. In *Modern Aspects of Electrochemistry*; Conway, B. E., Bockris, J. O'M., Eds.; Butterworths Scientific Publications: London, 1956 and references therein. Also Kebarle P. *Ann. Rev. Phys. Chem.* **1977**, *28*, 445−476.

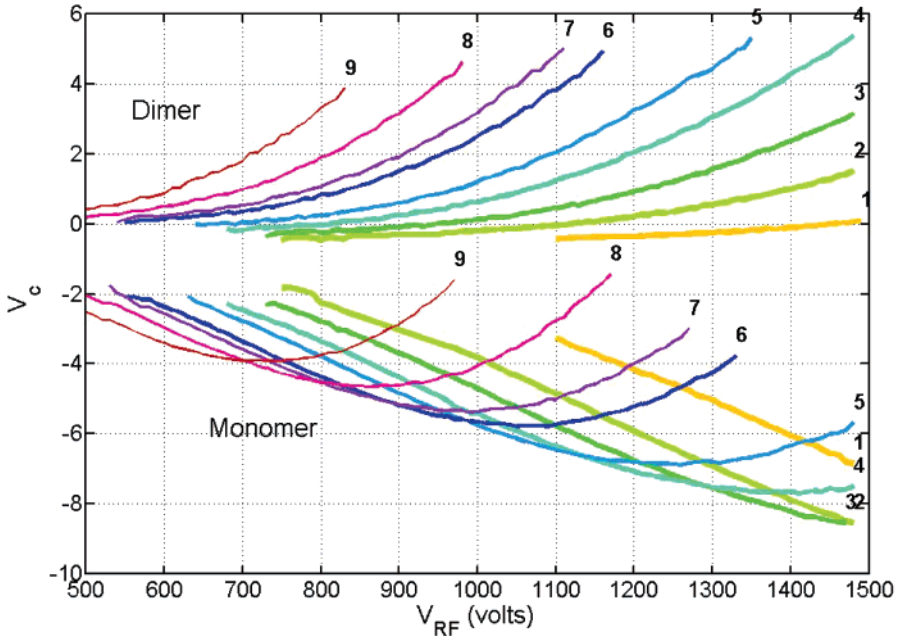

Figure 3. DMMP dimer and monomer peak positions at 35 °C for a range of pressures. Curves labeled 1−9 were recorded with sensor pressure values 1.555, 1.185, 1.006, 0.859, 0.764, 0.638, 0.592, 0.512, and 0.422 atm, respectively.

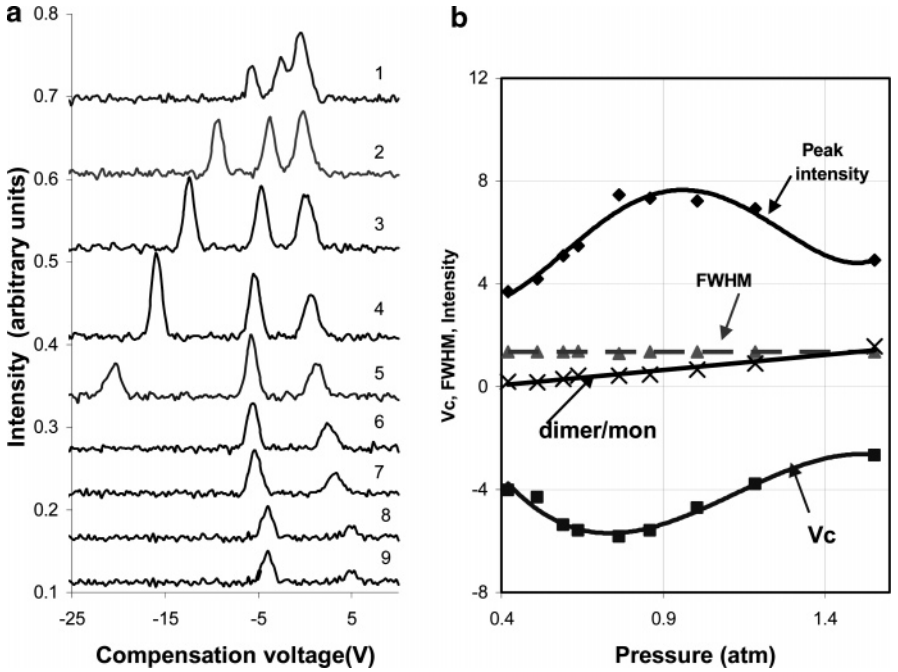

Figure 4. Effect of pressure on DMMP peak spectra (a) and peak parameters (b) for the protonated monomer peak at separation voltage of 1000 V. Spectra in (a) labeled 1−9 were recorded with sensor pressure values 1.555, 1.185, 1.006, 0.859, 0.764, 0.638, 0.592, 0.512, and 0.4 22 atm, respectively.

these pressures, the DMS provides peak intensity close to the maximum value and the best resolving power. In addition, the ratio of peak intensities for the protonated monomer and proton-bound dimer demonstrates that decreasing the pressure also decreases the formation of cluster ions, evident from an enhanced intensity of the monomer peak. Monomer ion peak position provides more reliable chemical identifications than cluster ion positions because cluster ions usually exhibit lower compensation voltage magnitudes ($|V_C|$) than monomers. The presence of a few clusters peaks near $V_C \sim 0$ V decreases the analytical space because poorly resolved cluster ions cannot be fully identified by peak position.

Consequently, the production of unclustered protonated monomer peaks through the regulation of pressure in a DMS analyzer provides a fast means of controlling response. Temperature regulation, by comparison, will be relatively slow owing to the thermal mass of existing technologies.

While compensation voltage and intensity were both affected by pressure, peak width was largely independent of changes in pressure as shown in Figure 4b. This is possible only when the

ratio is unchanged between transverse (rf driven) and longitudinal (transport flow driven) ion motion. The effect of pressure on linear velocity of ions in the analytical gap begins with a calculation of the number of drift gas molecules N inside the sensor volume V as proportional to pressures P_1 and P_2 at constant temperature (eqs 6a and b):

$$N_1 = P_1 V/kT \tag{6a}$$

$$N_2 = P_2 V/kT \tag{6b}$$

In this work, the same mass flow rate is maintained through the analyzer ($F = \Delta N/\Delta t = \text{const}$) and so variations in pressure will alter residence time by eq 7:

$$N_1/\tau_1 = N_2/\tau_2 \tag{7}$$

The combination of eqs 6 and 7 shows that residence time and pressure (or molecules density) are related per eq 8:

$$\tau_2 = (P_2/P_1)\tau_1 = (n_2/n_1)\tau_1 \tag{8}$$

Thus, the residence time of ions τ at a constant gas flow rate changes proportional to pressure in a DMS analyzer. A reasonable assumption is that longitude velocity of an ion is the same as that of the transport gas $\vartheta_{||} = L/\tau_r$ and linear velocities of ions for two pressures can be compared as in eqs 9a and b:

$$\vartheta_{||1} = L/\tau_1 \tag{9a}$$

$$\vartheta_{||2} = L/\tau_2 = \vartheta_{||1}(n_1/n_2) \tag{9b}$$

So, ion velocity is inversely proportional to gas density $\vartheta_{||2}/\vartheta_{||1} = n_1/n_2$. Thus, at lower pressure ($n_2 < n_1$), the longitude velocity of ions is higher than under higher pressure conditions ($\vartheta_{||2} > \vartheta_{||1}$).

The second component to this discussion of line broadening is the effect of pressure on transverse ion motion, which occurs due to the rf field. According to eq 8 of ref 16, ion transverse displacement due to the rf voltage is $Y = (\beta\Delta K/T)\tau$, where β corresponds to the area under the rf waveform in the high-field and low-field portions, ΔK is the difference of mobility coefficients at high and low electric fields, T is the rf waveform period, and τ is the residence time. Only certain ion species will survive passage through the analytical gap, those with displacement less than gap height G during the residence time. The maximum transverse ion drift velocity is thus

$$\vartheta_{\perp 1} = G/\tau_1 = \beta\Delta K_1/T \tag{10}$$

At other pressures, residence time τ_2 for the ions will be changed according (8). Therefore, from eq 10, leading to a new condition for ion survival at the same gap at the new pressure shown in eq 11

$$\vartheta_{\perp 2} = \frac{G}{\tau_2} = \frac{GP_2}{\tau_1 P_1} = \vartheta_{\perp 1}\frac{n_1}{n_2} \tag{11}$$

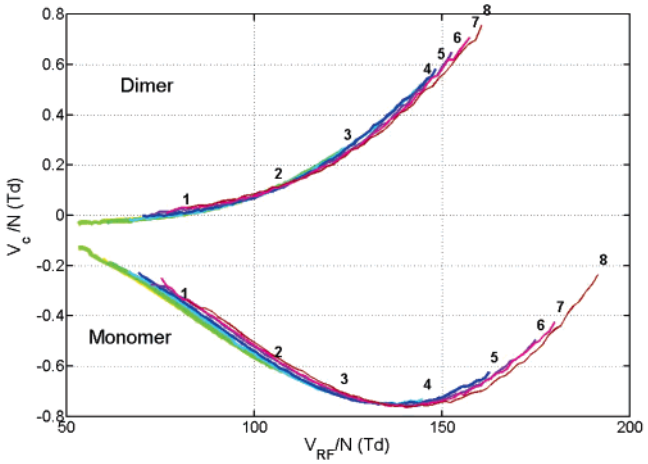

Figure 5. Townsend-scaled DMMP dimer and monomer peak positions at 35 °C for a range of pressures. The curves labeled 1−8 were recorded with sensor pressure values 1.555, 1.185, 1.006, 0.859, 0.764, 0.638, 0.592, and 0.512 atm, respectively.

From eq 11, it can be seen that pressure inversely affects ion velocity in the transverse direction. The pressure dependences of longitudinal (eqs 4a, b) and perpendicular direction velocities (eqs 5, 6) are thus the same:

$$\vartheta_{||2}/\vartheta_{\perp 2} = \vartheta_{||1}/\vartheta_{\perp 1} \tag{12}$$

In eq 12, ions are seen to have a similar relationship between longitude and transverse velocities, meaning that the slopes of effective trajectories are unchanged with pressure. Consequently, the effective trajectories and the peak width are the same for different pressures. The spectra in Figure 4a and plot for fwhm Figure 4b are consistent with this conclusion.

According to eq 1, the coefficient of mobility depends on E/N so that either pressure or field strength changes can cause a similar result when the other term is held constant or even when the other is changed in a supporting manner. We converted Figure 3 data to the Townsend-scale presentation.

This is shown in Figure 5 where a series of experiments with pressure are presented using Townsend unit scaling (E/N, 1 Td $= 10^{-21}$ V m^2) for both rf voltage and compensation voltage. Two conclusions can be drawn from this rescaling: first, all curves from Figure 3 fall on two universal curves, one curve for the monomer and one for the dimer, and second, the use of lower pressure has extended experimental DMS observations to much higher field values (up to $E/N \sim 200$ Td) using the same electronics. In Figure 5, an optimum E/N=140 Td value is evident that gives the best resolution, at the experimental temperature of 35 °C. This is evidence that binary collisions dominate even at the highest pressures reached in this experiment for both monomer and dimer ion species. Nonmonotonic behavior of this universal plot for monomer DMMP ions is understood as representing a transition between two mechanisms of ion−molecular interaction with increasing ion−neutral collision energy. In the case of DMMP ions in air before 140 Td, the coefficient of mobility increases with increasing energy of ions ($V_C \propto \alpha(E/N)$-according to ref 1), but afterward the process of decreasing of the coefficient mobility is observed. The nonsymmetric behavior

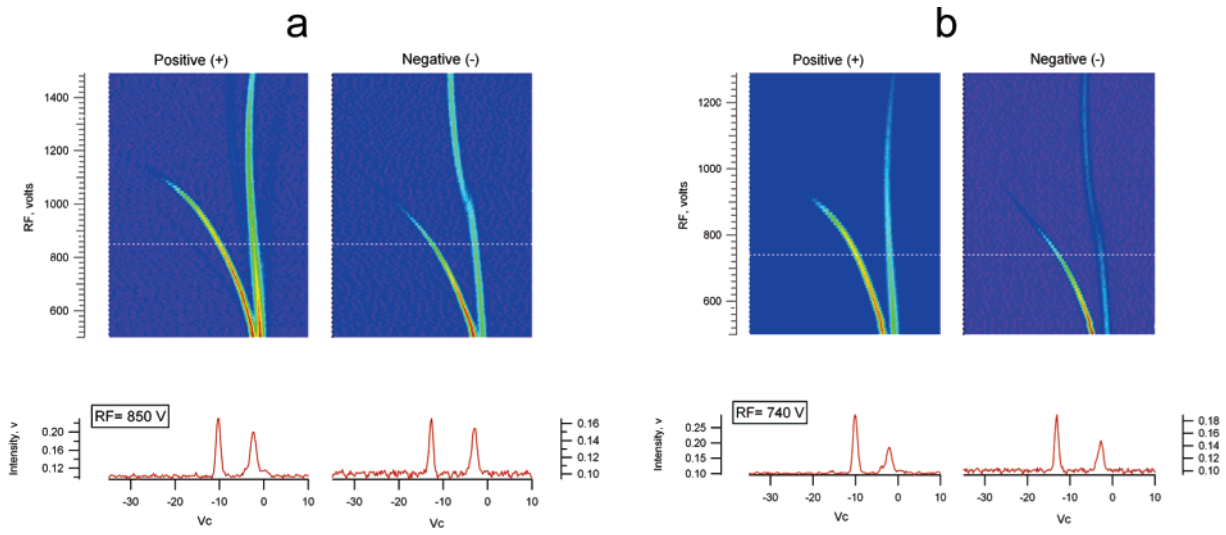

Figure 6. Dispersion plots for methyl salicylate in positive (left plots) and negative (right plots) polarity at pressures of 0.84 (a) and 0.65 atm (b).

of these curves suggest that the transformation of this curves reflects a process of transformation from elastic scattering due to polarization interaction to rigid-sphere ion−neutral interaction or resonance charge transfer. Consequently, monomers of DMMP exhibit a maximum for resolution at E/N of 140 Td with our waveform. This condition is independent of how E/N was reached, by regulation of pressure, by varying the electric field, or by simultaneous adjustment of both. The universal nature of this curve demonstrates the similarity of events occurring through ion−molecular interactions over our pressure range, allowing the plot to be used to predict the optimum separation field for DMMP ions. For example, at the highest experimental pressure (1.55 atm), the optimal value $E/N = 140$ Td can be attained with 37 500 V/cm corresponding to 1870 V with a 0.5-mm gap. Since our rf generator provides a maximum rf of 1500 V, we were unable to reach 140 Td for the highest pressures (curves1−3 in Figure 3), and only monotonic behavior of V_C as a function of V_{rf} was recorded. At lower pressures (curves 4−9), 1500 V exceeded the critical field for DMMP of $E/N = 140$ Td; therefore, curves show a maximum V_C magnitude. This critical E/N value will depend on the ion−molecule pair. Other ion species are expected to show different behavior and different critical points in universal E/N plots.

Methyl Salicylate. Formation of methyl salicylate ion species is well-documented in IMS.[36] Methyl salicylate forms positive and negative ions simultaneously in air at ambient pressure, offering insight into both negative and positive ion chemistry. Positive ions are formed as proton adducts, while methyl salicylate anions are formed as adducts with O_2^- resulting in $M{\cdot}O_2^-$ product ions. Since O_2^- adducts may have different binding energies and fragmentation pathways than $M{\cdot}H^+$, the effects of collision energy from the rf field on negative ions is expected to differ from that of positive polarity. DMS spectra were obtained for methyl salicylate in air at 10 pressures from 1.57 to 0.42 atm. The results for two of those pressures are shown as dispersion plots in Figure 6a and b for both polarities. Dispersion plots in each polarity show only two tracks, one for the reactant ion peak $H^+(H_2O)_n$ in positive polarity, and $O_2^-(H_2O)_n$ in negative polarity, and product ion at each rf value for each polarity. Positive ions tracks are smooth while the negative ion tracks have some irregularity at both pressures shown in Figure 6.

A distortion or break in the negative ion track is evident at 1020 V at 0.84 atm and 830 V at 0.65 atm, and the location of this point is dependent on pressure. At the highest pressures used here, a break point was not observed; however, the point became visible at 1350 V for a pressure of ~1.1 atm. The break point moved to smaller V_{rf} as pressure was reduced as shown in Figure 6 where a change of pressure by 0.19 atm, from 0.84 to 0.65 atm, caused a decrease in rf of 190 V, from 1020 to 830 V. Such breaks or irregular patterns are generally understood as chemical transformations under the strong electric field but must be confirmed by mass analysis of the ions.

Ion identities at various combinations of pressure and separation voltage were studied using DMS/MS. The DMS was used as a prefilter for a time-of-flight mass spectrometer, allowing ions from any part of the tracks shown in Figure 6 to be selected into the mass spectrometer.

When compensation voltage is adjusted to pass the positive reactant ions (left tracks), the mass spectra contain hydrated protons with m/z of 19 and 37 Da corresponding to $H^+(H_2O)_n$ for n of 1 and 2, respectively, along with some HN_2^+ (29 Da). These are the typical background ions for dry air. Suppression of chemical noise by the DMS prefilter is complete. Measurement with a compensation voltage away from any DMS ion peak shows no detectable ions in the mass spectrometer. In negative polarity, the reactant (background) ions were mass identified as oxygen anion, O_2^- (32 Da) and the hydrated anion $O_2^-H_2O$ (50 Da).

The product ions' mass spectra for methyl salicylate are shown in Figure 7 for positive (a) and negative (b, c) polarity ions. In positive mode, the peak contains only single ion species with m/z of 153 Da, the protonated monomer of methylsalicylate, MH^+. Increasing V_{rf} up to 1500 V, or E/N up to the maximums shown in the figure, did not alter the ion identity and affected only the ion intensity. In negative mode, (Figure 7b,c), the product ion at

(36) Eiceman, G. A.; Snyder, A. P.; Blyth, D. A. *Int. J. Environ. Anal. Chem.* **1990**, *38*, *415*−25.

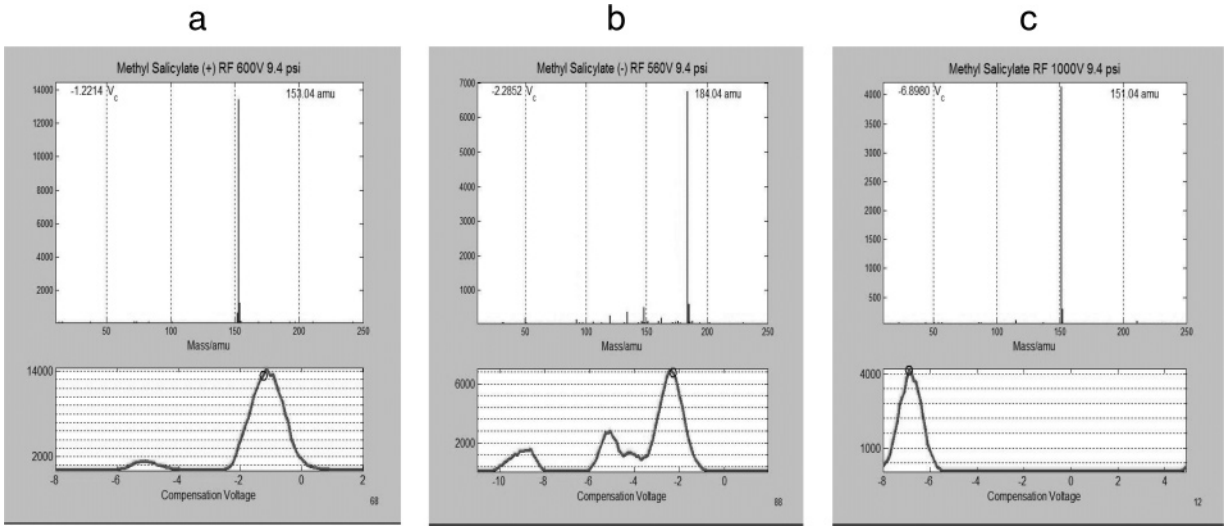

Figure 7. Mass spectra for ions from peaks in differential mobility spectra for methyl salicylate in positive polarity (a) and negative ions (b, c). The differential mobility spectra show the positive product ion (MH^+) (a), negative product ion before ($M{\cdot}O_2^-$) (b), and after $(M - H)^-$ (c) the break in tracks of the dispersion plot.

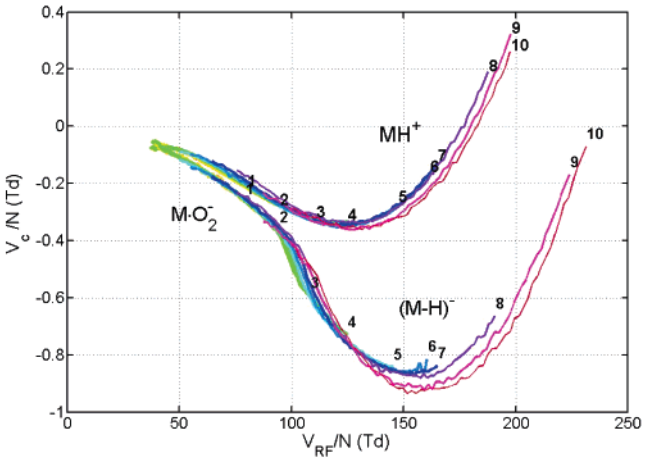

Figure 8. Methyl salicylate positive and negative ion Townsend-scale peak positions at a range of pressures. Curves labels 1−10 were recorded at pressures 1.55, 1.325, 1.132, 1.001, 0.838, 0.764, 0.652, 0.555, 0.480, and 0.421 atm. Mass spectral analysis has shown that in positive mode only the protonated methyl salicylate molecules are observed. In negative mode, the ion species at low *E*/*N* is the oxygen anion adduct and at high *E*/*N* the deprotonated monomer.

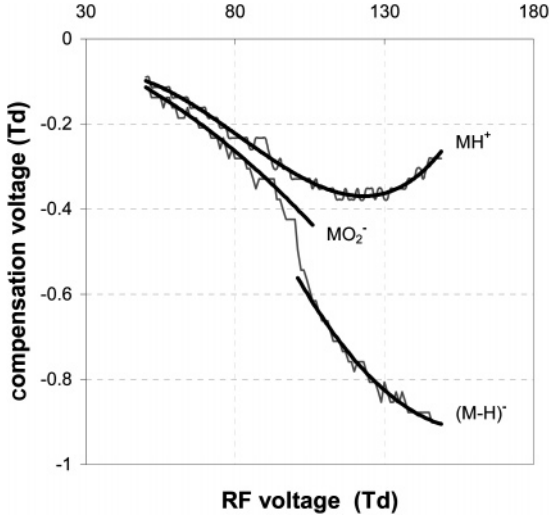

Figure 9. Example of transformation of methyl salicylate ions from MO_2^- to $(M - H)^-$ under the effect of rf voltage when *E*/*N* reaches a value of ~100 Td. Solid dark curves were obtained due by deconvoluting peak positions from experimental spectra (lighter traces) recorded at 0.838 atm. (curve 5 in Figure 8). Under the same conditions, positive protonated methyl salicylate ions are more stable and thus remain unchanged.

low V_{rf} showed an ion of m/z 184 Da, which we assign by exact mass as the adduct ion $M{\cdot}O_2^-$. At V_{rf} values after the transition in the traces of the dispersion plot, the ion seen in the mass spectrometer changes to m/z of 151 Da, the proton-abstracted $(M - H)^-$ ion. This ion arises from decomposition of the $M{\cdot}O_2^-$ by loss of an acidic hydrogen to O_2 through heating of the ion.[37] Plots of V_C versus V_{rf} in Townsend units, as given previously for DMMP, are shown for methyl salicylate in Figure 8 for positive (upper curves) and negative (bottom curves) ions.

A difference in minimum position is seen in these plots for the MH^+ and $M{\cdot}O_2^-$ ions. The optimum values for each polarity ions are 130 Td for MH^+ and 158 Td $(M - 1)^-$, even though these ion species are formed from the same molecule. And these values contrast with E/N of 140 Td for DMMP. While these differences are evident from the plots, the maximums are broad and conclusions on the importance of the differences are premature with measurements on only a few chemicals. On the other hand the center of the transition from $(M - H)^-$ to $M{\cdot}O_2^-$, always occurs in the range from 100 to 110 Td, as seen in Figure 8.

In Figure 9 we present a more detailed analysis of the ion transformation for the experimental data at 0.84 atm. The lighter traces show the experimental peak positions for the 100 separate V_C scans for rf values from 500 to 1500 V. The dark lines show peak positions determined by a deconvolution process. To calculate the deconvoluted peak positions, we used PeakFit software, assuming that detected peaks are the combination of two peaks with the same shape. This plot shows a transition from $M{\cdot}O_2^-$ to $(M - H)^-$ over a range in which the field increases from 98 to 105 Td. This may be understood in terms of increased

(37) Eiceman, G. A.; Bergloff, J. E.; Rodriquez, J. E.; Munro, W.; Karpas, Z. *J. Am. Soc. Mass. Spectrom.* **1999**, *10*, 1157−65.

collision energy or increased effective temperature. To induce loss of HO_2 from $M{\cdot}O_2^-$, the complex must gain between collisions enough kinetic energy to overcome the barrier to HO_2 elimination and subsequent rearrangement of the ion. Ions gain the required energy from the electric field between collisions. The kinetic energy is increased either by increasing the path between collisions, by reducing pressure, or by increasing the electric field strength to impart additional kinetic energy over the same path.

CONCLUSIONS

We suggest E/N scaling as a standardized presentation of DMS spectra, which enables comparison of spectra obtained under different experimental conditions (in this work for different pressures) and even in various sensor designs, because Townsend-scaled curves reveal the fundamental character of ion- molecular interactions.

Optimizing DMS performance requires that a balance be struck among several properties, including peak intensity, peak position (V_C), level of dimerization, peak width, transport gas breakdown voltage, and power consumption. Based on the data in Figure 4, we estimate that pressures in the 0.6−0.8 atm range provide reduced dimerization and high resolution. We have seen that DMS spectra of monomer ions in DMS often show the greatest compensation voltages, leading to the greatest peak capacity, at quite high separation field strengths, considerably above 100 Td in some cases. Because electric fields in DMS are extremely high, approaching the breakdown voltage of typical carrier gases, it may not be possible to apply the high required fields at higher pressures, especially with appropriate engineering derating factors. Breakdown voltage is highly dependent on electrode geometry, but for parallel-plate geometries, air breakdown parameters (Paschen's curve) are given in Bazelyan and Raizer.[38] Because Paschen's curve is sublinear near 1 atm, higher E/N values can be achieved at reduced pressure. Approximately a 15% increase in E/N can be achieved by reducing the operating pressure from 1 to 0.5 atm, and the required peak voltage is reduced by a factor of 2.

For portable DMS devices, low pressure is especially helpful. Generation of the asymmetric field rf waveform is a large part of the DMS power budget, even when efficient fly-back rf generators like that described by Krylov are used.[39] Since power consumption is proportional to the square of the voltage, $W \propto V^2$, operation at high voltage significantly increases power requirements. Using low pressure allows lower peak voltages, resulting in power savings. In Figure 2a, b, one can see that a monomer peak position of $V_C = -6.73$ V requires $V_{rf} = 1470$ V at elevated pressure (1.55 atm), while only 1200 V is needed at 0.76 atm. Comparing these spectra also shows that low pressure provides higher separation between the dimer and monomer peaks and decreases the dimer fraction for the same sample concentration. In summary, we find that operating DMS instruments at pressures below 1 atm provides reduced clustering and good monomer intensities, high V_C values, reduced chance of electrical breakdown for the certain E/N value, and reduced power consumption.

ACKNOWLEDGMENT

We thank Muning Zhong of Sionex for his valuable assistance with the experimental measurements, and Dr. Quan Shi of Sionex for assistance in data processing and data presentation.

Received for review June 15, 2006. Accepted September 12, 2006.

AC061092Z

(38) Bazelyan, E. M.; Raizer, Yu. P. *Spark Discharge*; CRC Press: Boca Raton, FL, 1998; p 39.

(39) Krylov, E.V. *Instruments and Experimental Techniques* **1997**, *40* (5), 628−31. (Translated from Russian.)